

2. INSTRUMENTATION AND SAMPLE PREPARATION

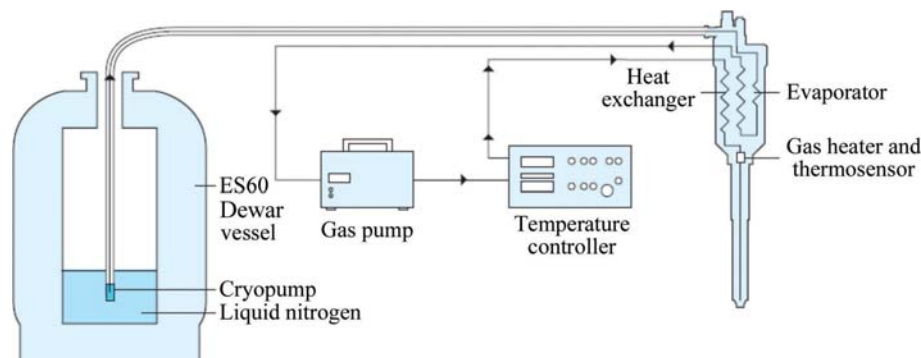


Figure 2.6.8
Schematic drawing of the Oxford Cryosystems cryostream setup.

cycle cryostat. This has the disadvantage that it consumes relatively large amounts of energy, but it does not need a continuous flow of helium and is also easy to use. The PheniX cryostat from Oxford Cryosystems is an example of such a chamber, which makes it possible to cool flat-plate powder samples to 20 K in just 35 min and to as low as about 12 K after a further 25 min. Recently, a group using beamline L11 at the Diamond Light Source synchrotron made some modifications to the PheniX cryostat to enable it to perform low-temperature Debye–Scherrer powder diffraction (Potter *et al.*, 2013). The original flat-plate sample holder in the cryostat was changed to a capillary sample holder.

2.6.7.2. Cryogenic cooling stages/cryostream

The cryostream from Oxford Cryosystems (Cosier & Glazer, 1986) cools the sample in a different way (Fig. 2.6.8). Originally developed for single-crystal X-ray diffraction experiments, it is currently also used to cool/heat capillaries in Debye–Scherrer experiments (Fig. 2.6.9). To prevent atmospheric moisture from freezing on the capillary, the cryogenic nitrogen-gas stream is shrouded in a second dry gas stream. When the two flows are balanced, the outer stream protects the inner nitrogen stream and temperatures as low as 80 K can be reached without ice forma-

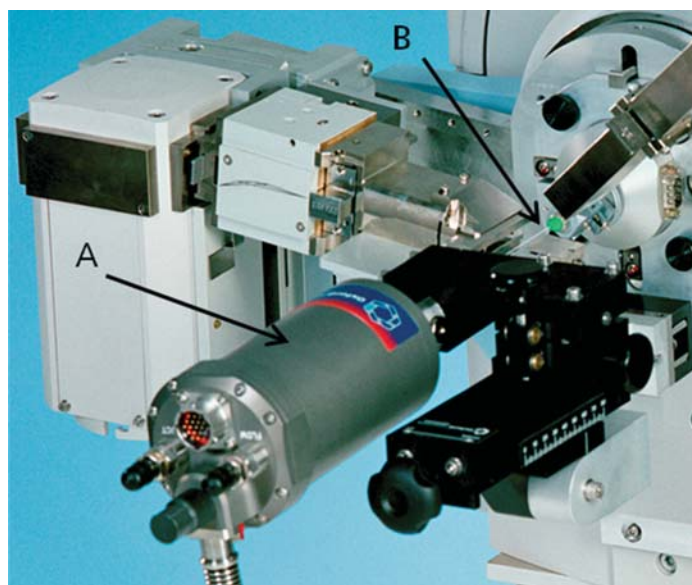


Figure 2.6.9
Oxford Cryostream (A) mounted on a PANalytical diffractometer for cooling a capillary (B).

tion on the capillary. The main advantage of measuring a powder sample in a capillary (transmission geometry) in contrast to flat-plate reflection geometry is minimization of preferred orientation of the sample. Attention must be paid, as in all non-ambient measurements, to temperature gradients in the sample. A short capillary is therefore advisable to minimize the occurrence of a gradient along the capillary.

For absorbing samples, hard radiation must be used to completely penetrate the capillary. Another possibility is to use capillaries with very small diameters, but this is not always very easy and filling them can be time consuming.

Example: buckminsterfullerene. An example that demonstrates the capability of the pair distribution function (PDF) method to independently probe the short-range and long-range atomic ordering in materials is C_{60} , also known as $(C_{60-I_h})[5,6]$ fullerene, fullerene or buckyball (Egami & Billinge, 2003). A buckyball molecule consists of 60 C atoms arranged on the vertices of a soccer-ball-like frame. At room temperature the C_{60} molecules are arranged in a face-centred cubic (f.c.c.) lattice and they assume completely random orientations as a result of thermal energy.

For long-range atomic order to be present, the atoms of the C_{60} molecules must remain in the same crystallographic position, which is not the case at room temperature. The time-averaged structure of the material can be represented as an f.c.c. structure, with space group $Fm\bar{3}m$, of uniform hollow balls with a diameter of about 7.1 Å. On cooling through 260 K a first-order structural phase transition occurs; the random rotation of each C_{60} molecule becomes slower and is now best described as a librational motion (Brown *et al.*, 2005). The phase transition is accompanied by a sudden contraction of the cubic lattice parameter and the long-range order can be described with a primitive cubic lattice (space group $Pa\bar{3}$).

Fig. 2.6.10 shows the atomic PDF at room and low temperature; only the short distances within the balls are clearly observed at room temperature (Reiss *et al.*, 2012). The correlation between atoms of neighbouring molecules cannot be seen, but ball–ball correlations are visible at larger distances. The low-temperature measurement shows similar peaks below 7.1 Å as the ambient measurement, but above 7.1 Å peaks are visible that result from distances from C atoms in one C_{60} molecule to C atoms in another C_{60} molecule.

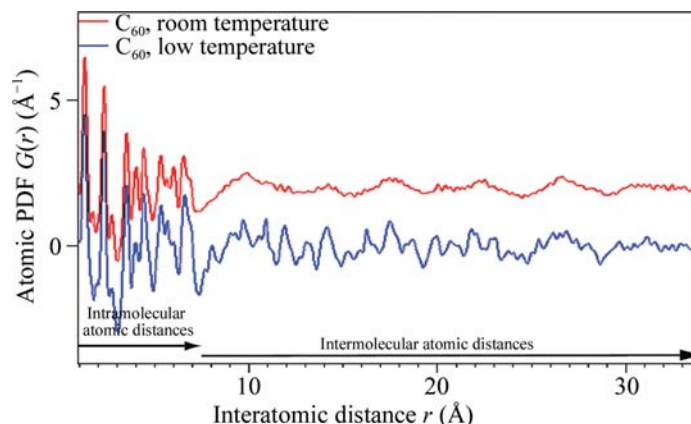


Figure 2.6.10
Atomic pair distribution function of C_{60} at room temperature (red) and at 100 K (blue).

2.6. NON-AMBIENT-TEMPERATURE POWDER DIFFRACTION

2.6.8. Temperature accuracy

The accuracy of the temperature measurement of a non-ambient device has to be determined before starting a non-ambient experiment. At present no certified temperature standards for X-ray powder diffraction are available, only commonly used reference materials. A list of these materials can be found at <https://www.xrayforum.co.uk/> and https://bl831.als.lbl.gov/~jamesh/pickup/Snell_SG_change_table.pdf.

A common method for validation of a non-ambient chamber is by determining the thermal expansion coefficient of a reference material as a function of temperature. Another is to determine the transition temperature of well known phase transformations. A third method is the so-called 'differential thermal expansion' method (Drews, 2001). This method utilizes the relative thermal expansion of two diffraction peaks. These peaks can be from the same or different reference material(s) but must be found in a narrow angular range and have different thermal expansion behaviour. Using only the relative separations of the peaks that are closely spaced eliminates the need for full pattern refinement to take into account geometrical aberrations and makes this method fast.

2.6.9. Future

A whole new field of non-ambient experiments has opened up with the study of new applications such as non-ambient PDF (see Section 2.6.7.2) and non-ambient SAXS measurements. And what happens in the nano world when large-scale models no longer hold at ambient and non-ambient temperatures? The future will tell; non-ambient diffraction/scattering experiments are more relevant now than ever before.

References

Angelkort, J., Apostolov, Z. D., Jones, Z. A., Letourneau, S. & Kriven, W. M. (2013). *Thermal properties and phase transition of $2\text{ZrO}_2\cdot\text{P}_2\text{O}_5$ studied by in situ synchrotron X-ray diffraction*. *J. Am. Ceram. Soc.* **96**, 1292–1299.

Brown, C., Copley, J. & Qiu, Y. (2005). *The orientational order/disorder transition in buckminsterfullerene (C_{60}): an experiment using the NCNR Disk Chopper Spectrometer*. Gaithersburg: NIST Center for Neutron Research. https://www.ncnr.nist.gov/summerschool/ss05/C60_EXPT_05.pdf.

Butté, R., et al. (2007). *Current status of AlInN layers lattice-matched to GaN for photonics and electronics*. *J. Phys. D Appl. Phys.* **40**, 6328–6344.

Cosier, J. & Glazer, A. M. (1986). *A nitrogen-gas-stream cryostat for general X-ray diffraction studies*. *J. Appl. Cryst.* **19**, 105–107.

Daillant, J. & Gibaud, A. (2009). Editors. *X-ray and Neutron Reflectivity: Principles and Applications*. Berlin, Heidelberg: Springer.

Drews, A. R. (2001). *Calibration of a high temperature X-ray diffraction stage by differential thermal expansion*. *Adv. X-ray Anal.* **44**, 44–49.

Egami, T. & Billinge, S. J. L. (2003). *Underneath the Bragg Peaks: Structural Analysis of Complex Materials*. Oxford: Pergamon.

Grieger, L., Kharchenko, L., Heuken, M. & Woitok, J. F. (2013). *15th European Workshop on Metalorganic Vapour Phase Epitaxy (EWMOVPE XV)*, Extended abstracts, pp. 51–54. Jülich: Forschungszentrum Jülich.

Kelekci, O., Tasli, P., Cetin, S. S., Kasap, M., Ozcelik, S. & Ozbay, E. (2012). *Investigation of AlInN HEMT structures with different AlGaIn buffer layers grown on sapphire substrates by MOCVD*. *Curr. Appl. Phys.* **12**, 1600–1605.

Norby, P. & Schwarz, U. (2008). *Powder Diffraction: Theory and Practice*, edited by R. E. Dinnerbier & S. J. L. Billinge, pp. 439–463. Cambridge: Royal Society of Chemistry.

Odler, I. (2000). *Special Inorganic Cements*. London: CRC Press.

Potter, J., Parker, J. E., Lennie, A. R., Thompson, S. P. & Tang, C. C. (2013). *Low-temperature Debye–Scherrer powder diffraction on Beamline I11 at Diamond*. *J. Appl. Cryst.* **46**, 826–828.

Reiss, C. A., Kharchenko, A. & Gateshki, M. (2012). *On the use of laboratory X-ray diffraction equipment for pair distribution function (PDF) studies*. *Z. Kristallogr.* **227**, 256–261.

Sarin, P., Yoon, W., Jurkschat, K., Zschack, P. & Kriven, W. M. (2006). *Quadrupole lamp furnace for high temperature (up to 2050 K) synchrotron powder X-ray diffraction studies in air in reflection geometry*. *Rev. Sci. Instrum.* **77**, 092906.

Teke, A., Gökden, S., Tülek, R., Leach, J. H., Fan, Q., Xie, J., Özgür, Ü., Morkoç, H., Lisesivdin, S. B. & Özbay, E. (2009). *The effect of AlN interlayer thicknesses on scattering processes in lattice-matched AlInN/GaN two-dimensional electron gas heterostructures*. *New J. Phys.* **11**, 063031.

Weast, R. C. (1980). *CRC Handbook of Chemistry and Physics*, 61st ed. Boca Raton: CRC Press.